Mol Biol Rep (2015) 42:1123–1138
DOI 10.1007/s11033-015-3850-5

Immuno-affinity purification of *Pgl*PGIP1, a polygalacturonase-inhibitor protein from pearl millet: studies on its inhibition of fungal polygalacturonases and role in resistance against the downy mildew pathogen

Sreedhara Ashok Prabhu · Martin Wagenknecht · Prasad Melvin · Belur Shivappa Gnanesh Kumar · Mariswamy Veena · Sekhar Shailasree · Bruno Maria Moerschbacher · Kukkundoor Ramachandra Kini

Received: 11 July 2014 / Accepted: 9 January 2015 / Published online: 18 January 2015

Abstract Polygalacturonase-inhibitor proteins (PGIPs) are important plant defense proteins which modulate the activity of microbial polygalacturonases (PGs) leading to elicitor accumulation. Very few studies have been carried out towards understanding the role of PGIPs in monocot host defense. Hence, present study was taken up to characterize a native PGIP from pearl millet and understand its role in resistance against downy mildew. A native glycosylated PGIP (*Pgl*PGIP1) of ~43 kDa and pI 5.9 was immunopurified from pearl millet. Comparative inhibition studies involving *Pgl*PGIP1 and its non-glycosylated form (r*Pgl*PGIP1; recombinant pearl millet PGIP produced in *Escherichia coli*) against two PGs, PG-II isoform from *Aspergillus niger* (*An*PGII) and PG-III isoform from *Fusarium moniliforme*, showed both PGIPs to inhibit only *An*PGII. The protein glycosylation was found to impact only the pH and temperature stability of PGIP, with the native form showing relatively higher stability to pH and temperature changes. Temporal accumulation of both *Pgl*PGIP1 protein (western blot and ELISA) and transcripts (real time PCR) in resistant and susceptible pearl millet cultivars showed significant *Sclerospora graminicola*-induced accumulation only in the incompatible interaction. Further, confocal PGIP immunolocalization results showed a very intense immuno-decoration with highest fluorescent intensities observed at the outer epidermal layer and vascular bundles in resistant cultivar only. This is the first native PGIP isolated from millets and the results indicate a role for *Pgl*PGIP1 in host defense. This could further be exploited in devising pearl millet cultivars with better pathogen resistance.

Keywords Chemical deglycosylation · Confocal immunolocalization · Peptide mass fingerprinting · Plant–pathogen interaction · Quantitative real-time PCR · Two-dimensional gel electrophoresis

Electronic supplementary material The online version of this article (doi:10.1007/s11033-015-3850-5) contains supplementary material, which is available to authorized users.

S. A. Prabhu · P. Melvin · M. Veena · K. R. Kini (✉)
Department of Studies in Biotechnology, University of Mysore, Manasagangotri, Mysore 570 006, Karnataka, India
e-mail: krk@appbot.uni-mysore.ac.in

M. Wagenknecht · B. M. Moerschbacher
Institut für Biologie und Biotechnologie der Pflanzen, Westfälische Wilhelms-Universität Münster, Schlossplatz 8, 48143 Münster, Germany

B. S. Gnanesh Kumar
Protein Biochemistry and Glycobiology Laboratory, Department of Biochemistry, University of Hyderabad, Hyderabad 500046, Andhra Pradesh, India

S. Shailasree
Institution of Excellence, Vijnana Bhavan, University of Mysore, Manasagangotri, Mysore 570 006, Karnataka, India

Introduction

The plant cell wall (CW) which acts as both a rigid structural embankment as well as a flexible layer during cell expansion has evolved into a complex network of polysaccharides such as cellulose, hemicellulose, pectin and proteins [1]. Due to their strategic position, CWs are crucial in plant–microbe interactions, including defense against phytopathogens [2]. Homogalacturonides (HGs) are linear, α-1,4-linked-D-galactopyranosyluronic acid chains, with a significant portion of the residues methyl esterified and/or acetylated, and constitute the "smooth region" of the complex pectin [3]. Polygalacturonases (PGs) are

known to be one of the first and most important virulence factors secreted by pathogens which degrade the HG [4]. Molecular studies have well established the role of both fungal and bacterial PGs in causing plant diseases [5–7]. Though not much was known till recently regarding the role of PGs in oomycetes, today, evidences display involvement of PGs in infection of plants by oomycetes such as *Phytophthora* spp. [8, 9].

The plants employ polygalacturonase-inhibitor proteins (PGIPs), CW glycoproteins belonging to the leucine-rich repeat protein superfamily to counter microbial onslaught by inhibiting/modulating PG activity [10]. PGIPs are known to inhibit PGs of fungal [11], insect [12] and bacterial origins [13] but are shown to be ineffective against those from plants [14]. PGIPs are known to directly suppress PG activity, in the process, favoring accumulation of elicitor active oligogalacturonides (OGs), and also contribute to pathogen perception by preventing the degradation of OG-elicitors [15, 16].

PGIPs have been extensively demonstrated to be involved in dicot host defense to pathogens and other environmental stresses. For example, in poplar and chilli, PGIP-encoding genes showed comparatively higher expression levels in incompatible interactions than in compatible ones [17, 18]. Differential regulation in gene expression and differential PG inhibition specificities of PGIPs from a single plant species in response to pathogens and other abiotic/biotic elicitors has been considered to be critical in mounting an effective host defense [10, 19]. Transgenic *pgip* overexpression studies have shown the direct relationship between the protein levels and reduction in disease severity against both fungal and bacterial pathogens in plants such as tomato, tobacco, *Arabidopsis*, and Chinese cabbage [20–24]. In addition, importance of the inhibitor in *Arabidopsis* innate immunity was demonstrated by the increased susceptibility to *Botrytis cinerea* infection by plants expressing *pgip* in antisense [25]. Comparatively, in monocot plants, very few studies have been carried out towards understanding the role of PGIPs in host defense and the studies have mainly been restricted to wheat and rice [24, 26–31].

Pearl millet (*Pennisetum glaucum* [L.] R. Br.; synonym: *Cenchrus americanus* (L.) Morrone) is the sixth most important cereal crop in the world grown for forage, grain and stover in drought-prone regions of the arid and semi-arid tropics of Africa and South Asia [32, 33]. Downy mildew caused by the obligate biotroph *Sclerospora graminicola* is still the major biotic limitation in pearl millet production [34]. Efforts such as application of biotic/abiotic elicitors [35, 36], conventional and marker-assisted generation of hybrids [37] and transgenic expression of defense genes have been made in pearl millet to counter the downy mildew [38]. However, breakdown of resistance has been observed against downy mildew in pearl millet hybrids grown in the same field for more than three consecutive crop seasons. This indicates the prevalence of high natural variation in pathogen population thus leading to emergence/selection of new virulence [39]. Hence, continuous efforts in the identification of additional markers and genes would be critical in future generation of pearl millet lines resistant to downy mildew. The present study is in continuation with our earlier attempt to purify PGIP from pearl millet and assess its role in the defense against the downy mildew disease [40–42]. Here, we have immunopurified a PGIP from pearl millet and explored its role in host defense against *S. graminicola*. In addition, the effect of PGIP glycosylation on PG inhibition [PG-II isoform from *Aspergillus niger* (*An*PGII) and PG-III isoform from *Fusarium moniliforme* (*Fm*PGIII)] has been explored using the native glycosylated and the non-glycosylated PGIP forms.

Materials and methods

Plant material, pathogen and inoculation

Pearl millet cultivars, IP18296 (highly resistant) and 7042S (highly susceptible) displaying downy mildew disease incidences of 0 % and >25 %, respectively, post inoculation with *S. graminicola* under field conditions were chosen for the present study. The seeds were obtained from International Crop Research Institute for Semi-Arid Tropics, Hyderabad, India.

Sclerospora graminicola isolated from pearl millet cv. HB3 maintained under greenhouse conditions was used for all inoculation experiments. Leaves displaying downy mildew symptoms were collected in the evening and previous sporangial crop was washed off under running tap water. Further, the leaves were blot-dried, down-sized to about 4 inch length and incubated overnight at 22 °C and relative humidity of >90 %. The following morning, the zoosporangia were harvested and the released zoospores were used as inoculum.

The seeds of IP18296 and 7042S cultivars were surface sterilized for 15 min in 0.1 % (w/v) sodium hypochlorite solution. Then rinsed thoroughly with sterile distilled water and germinated on moist filter paper under aseptic conditions in dark for 2 days at 25 ± 2 °C. Two-day-old seedlings were root-dip inoculated with 4×10^4 zoospores ml^{-1} of *S. graminicola*. The seedlings (ten seedlings of IP18296 and 7042S at each experimental time point of each study) were harvested at time intervals of 0, 6, 12, 24 and 48 h post inoculation (h.p.i.), frozen immediately in liquid nitrogen and stored at −80 °C until further use. Un-inoculated water-treated seedlings of both cultivars maintained in parallel served as controls.

Production and purification of *Pgl*PGIP1 and r*Fm*PGIII fusion proteins in *Escherichia coli*

The r*Pgl*PGIP1 (pearl millet PGIP1 fusion protein; MBP-IEGR-*Pgl*PGIP1-6xHis-Strep-tag® II; MBP, maltose-binding protein; 'IEGR', Factor Xa protease cleavage site; 6xHis, hexa histidine tag), rVC (vector control; MBP-IEGR-6xHis-Strep-tag® II), and r*Fm*PGIII (*Fusarium moniliforme* polygalacturonase isoform 3 fusion protein; *Fm*PGIII-Strep-tag® II) fusion proteins were produced in *E. coli* SHuffle® T7 Express [pLysSRARE2] and purified as described in Prabhu et al. [42]. The protein concentration was determined using the BCA protein assay kit (Pierce) with BSA as standard.

Production and purification of polyclonal antibody specific to a *Pgl*PGIP1 peptide

Identification of a highly immunogenic pearl millet PGIP peptide based on the deduced amino acid sequence of *Pglpgip1* (GenBank accession number (Acc. No.): JF421 287) representing residues 292–305 (CQTQLFNVSYNQ LCG), Keyhole limpet hemocyanin-conjugated peptide synthesis, its purification and mass spectrometry-based sequence confirmation, anti-peptide polyclonal antibody (Pab_{pep}-*Pgl*PGIP1) production in New Zealand white rabbits and IgG purification were carried out at Genosphere Biotechnologies (France).

Determination of Pab_{pep}-*Pgl*PGIP1 specificity by western blot analysis

Pab_{pep}-*Pgl*PGIP1 specificity was verified by immunoblot analysis against r*Pgl*PGIP1, total pearl millet protein (50 µg) and rVC (2 µg each). The possibility of antibody cross reactivity was investigated against crude protein extracts from various plants such as wheat, rice, sorghum, maize, French bean, tomato, potato, soybean, cotton and capsicum (50 µg each). In addition, antibody cross reactivity was investigated by including various unrelated proteins such as r*Fm*PGIII, *An*PGII, BSA, myosin, laminarin, RNase A and DNase I (2 µg each). The proteins were separated on 10 % sodium dodecyl sulfide-polyacrylamide gels. The separated proteins were blotted onto a polyvinylidene difluoride (PVDF) membrane using the Multiphor II (Pharmacia, Sweden) electrophoretic transfer apparatus according to the manufacturer's protocol. Overnight blocking of the blots was carried out with 5 % (w/v) blotting-grade milk powder in Tris-buffered saline (TBS: 10 mM Tris HCl, pH 8.0, 150 mM NaCl). The following day, the blots were washed with TBS buffer containing 0.05 % (w/v) Tween-20 (TBST), three times for 5 min each. The blots were then incubated with Pab_{pep}-*Pgl*PGIP1 (1:10,000 dilution in blocking buffer) for 90 min at 37 °C and washed five times with TBST. The blots were then incubated with goat anti-rabbit IgG conjugated with horseradish peroxidase (HRP; 1:20,000 in blocking buffer dilution) for 60 min at 37 °C. Finally, the membranes were washed thrice in TBST. The chemiluminescence detection of blots was carried out as mentioned previously [43]. The pre-immune serum was used to confirm absence of any cross-reactivity with PGIP.

Total protein extraction from IP18296 and 7042S seedlings

Total protein was extracted from 2-day-old IP18296 and 7042S (control and inoculated) samples harvested at 0, 6, 12, 24 and 48 h.p.i. according to the modified method of Favaron et al. [44]. All the steps were carried out at 4 °C. Briefly, 10 g plant tissue was homogenized in 2 volumes of ice-cold acetone and centrifuged at 15,000×*g* for 30 min. The pellet was washed twice with ice-cold acetone under the same conditions, air-dried completely and resuspended in 2 volumes of sodium acetate buffer (20 mM, pH 5.0 containing 1 M NaCl). The resuspended pellet was incubated at 4 °C for 72 h on a shaker to facilitate leaching out of wall bound proteins. The protein resuspension was centrifuged at 15,000×*g* for 30 min and the resulting supernatant was dialyzed against 20 mM sodium acetate buffer, pH 4.0. The dialyzed protein extract was lyophilized and appropriately reconstituted in suitable buffers. The protein concentration was determined using the BCA protein assay kit (Pierce) with BSA as standard.

Immuno-affinity purification of PGIP from IP18296 seedlings

An immuno-affinity resin of 2 ml capacity was prepared and packed in a glass column (5 × 1 cm) by attaching Pab_{pep}-*Pgl*PGIP1 (10 mg ml^{-1}) to cyanogen bromide activated Sepharose 4B (GE Healthcare Life Sciences) according to the manufacturer's instructions. The column was equilibrated with 10 bed volumes of 20 mM phosphate buffer, pH 7.0 containing 1 mM EDTA and 0.8 % (w/v) NaCl. Pearl millet total protein (extracted from 5 kg of 2-day-old IP18296 seedlings harvested 24 h.p.i.) reconstituted in the same buffer was loaded onto the column at a flow-rate of 10 ml h^{-1}. The column was loaded with 5 mg protein each time, washed intermittently and eluted with the same buffer containing 3 M potassium thiocyanate. The protein eluates were concentrated using centrifugal concentrators (Vivaspin™20, Sartorius) and reconstituted in suitable buffers and stored at 4 °C. The protein concentration was determined using the BCA protein assay kit (Pierce) against a BSA standard.

Two-dimensional (2D) gel electrophoresis of the purified protein

The purified protein (5 μg) was finally solubilized in suitable volumes of iso-electric focusing (IEF) buffer (8 M urea, 2 M thiourea, 0.5 % (w/v) ampholytes, 2 % (w/v) [(3-Cholamidopropyl)dimethylammonio]-1-propanesulfonate, 1 % (w/v) dithiothreitol (DTT) and 0.002 % (w/v) bromophenol blue). An immobilized pH gradient (IPG) strip (7 cm linear, pH 4.0–7.0, Bio-Rad Ready Strip) was actively rehydrated at 50 V for 12 h with a suitable volume of IEF buffer containing the protein and focused using a Protean IEF Cell (Bio-Rad, Germany) at 20 °C applying the following program: a linear increase from 0 to 500 V over 1 h, 500–1000 V over 1 h, 100–10,000 V over 2.5 h and then held at 10,000 V for a total of 60 kVh. Post focusing, the proteins were reduced by incubating the IPG strip with 1 % (w/v) DTT for 10 min. The strips were then transferred to 12 % sodium dodecyl sulfide-polyacrylamide gel for second dimension electrophoresis at 25 V applied for 1 h followed by 50 V using a Protean xi cell (Bio-Rad, Germany) with an attached cooling unit to maintain temperature of the unit at 16 °C, applied till the dye front reached the gel bottom. Gels were visualized by Coomassie Brilliant Blue R-250 staining.

Mass spectrometry (MS) analysis of the purified protein: peptide mass fingerprinting (PMF) using matrix-assisted laser desorption ionization time of flight/time of flight (MALDI-TOF/TOF) MS

The protein spot was excised from the 2D gel and subjected to in-gel proteolytic digestion with trypsin after reduction and alkylation according to the method described by Shevchenko et al. [45]. For MS analysis, the resulting tryptic peptides were reconstituted in 5 μl of 1:1 acetonitrile and 1 % trifluoroacetic acid. Two microlitres of this sample was mixed with 2 μl of freshly prepared α-cyano-4-hydroxycinnamic acid matrix in 50 % acetonitrile and 1 % trifluoroacetic acid (1:1) and 1 μl was spotted on the target plate. Mass spectra were obtained by use of an Autoflex III MALDI TOF/TOF instrument (Bruker Daltonics, Germany) equipped with smart beam laser (335 nm; 1,000 Hz) in the positive ion mode and the time-of-flight analyzer was operated in reflectron mode. Spectra were calibrated externally using a standard peptide mixture (angiotensin II [1046.5 Da], angiotensin I [1296.7 Da], substance P amide [1347.7 Da], bombesin [1619.8 Da], adrenocorticotrophic hormone (ACTH) fragment 1–17 [2093.1 Da], ACTH fragment 18–39 [2465.2 Da], and somatostatin 28 [3147.5 Da]) (Bruker Daltonics). The precursor peptide ions were fragmented using the LIFT.lft method (Bruker Daltonics) and the acquired data was searched against NCBInr with the automated database-searching program using the Mascot search engine version 2.4 (Matrix Science) employing Biotools software (Bruker Daltonics). The following parameters were applied for database search: database (NCBInr); taxonomy: Viridiplantae (green plants); proteolytic enzyme: trypsin; global modification: carbamidomethyl (C); variable modification: oxidation (M); peptide charge state: +1; and maximum missed cleavage: 1. According to the Mascot probability analysis ($p < 0.05$), only significant hits were accepted for protein identification.

Chemical deglycosylation and western blot analysis of total protein from IP18296 seedlings

Deglycosylation of total protein from 2-day-old IP18296 seedlings harvested at 24 h.p.i. was carried out according to the method of Edge et al. [46]. About 3 mg protein was dissolved in 135 μl of trifluoromethanesulfonic acid (TFMS) and 15 μl of anisole in a 0.3 ml vial and kept on ice for 2 h. The reaction mixture was added to 3 ml ice-cold pyridine:diethyl ether (1:9). The precipitated salts were collected by centrifugation at 4,000×*g* for 5 min at 4 °C, resuspended in 1 ml of 0.1 M NH_4HCO_3 and dialyzed against the same buffer. The resulting precipitated protein was pelleted by centrifugation at 12,000×*g* for 15 min at 4 °C. The protein concentration was determined using the BCA protein assay kit (Pierce) with BSA as standard.

SDS-PAGE and immunoblot analysis (using 1:10,000 dilution of Pab_{pep}-*Pgl*PGIP1 and 1:20,000 goat anti-rabbit IgG conjugated with HRP) of the untreated and chemically deglycosylated total proteins (50 μg each) were carried out as mentioned above.

PGIP activity assays

The purified native *Pgl*PGIP1 and recombinant r*Pgl*PGIP1 were assayed for inhibition of two fungal polygalacturonases—*An*PGII and r*Fm*PGIII as described in Prabhu et al. [42]. The rVC served as the negative control. *An*PGII (5 ng) and r*Fm*PGIII (36 ng) were incubated separately in a reaction volume of 200 μl with 0.1 mg ml^{-1} polygalacturonic acid substrate (Sigma) at 30 °C in 50 mM sodium acetate buffer, pH 4.2 and 4.6, respectively. PG activity was determined by reducing end-group analysis according to Anthon and Barret [47]. The PGIP activity was assayed by measuring the activity of the PGs pre-incubated with r*Pgl*PGIP1 for 20 min at 30 °C. The PGIP activity was expressed as per cent reduction in the number of reducing ends (in μkat mg^{-1} protein) liberated by PGs in the presence and absence of PGIP.

The effect of various parameters such as inhibitor concentration (0.316–12.64 nM *Pgl*PGIP1), substrate

concentrations (0.025–0.25 mg ml^{-1}) and pH (3.5, 4.0, 4.5 and 5.0) on enzyme inhibition was investigated. The kinetic parameters were computed by fitting the Michaelis–Menten equation on initial rate experimental data by non-linear fitting using OriginPro7 (Originlab). In separate experiments, the temperature and pH stability of the inhibitor protein was studied by pre-incubating them separately for 1 h at temperatures ranging from 20 to 100 °C and; for 16 h at pH values 2–11, at 4 °C, respectively, upon which they were reconstituted in the appropriate assay buffer and their inhibition potential was assayed at 30 °C.

Analyses of *Pgl*PGIP1 accumulation in IP18296 and 7042S seedlings by western blotting and ELISA

About 50 µg each of the total proteins extracted from 2-day-old IP18296 and 7042S (control and inoculated) samples harvested at 0, 6, 12, 24 and 48 h.p.i. was used for both western blot and ELISA studies. SDS-PAGE and immunoblot analysis (using 1:10,000 dilution of Pab_{pep}-*Pgl*PGIP1 and goat anti-rabbit IgG conjugated with HRP) were carried out as mentioned above. ELISA was carried out as described by Deepak et al. [48]. The antigen was coated onto 96-well microtiter plates (Nunc, Denmark) and the volume was made up to 100 µl $well^{-1}$ with antigen buffer (10 mM sodium acetate buffer, pH 3.6). The plates were incubated overnight at room temperature and then washed with 200 µl $well^{-1}$ wash buffer (phosphate buffered saline (PBS): 137 mM NaCl, 2.7 mM KCl, 10 mM phosphate buffer, pH 7.2 containing 0.5 % Tween-20). The wells were further blocked with 200 µl of blocking buffer (PBS containing 5 % skimmed milk powder) for 1 h at 37 °C. Post washing, the wells were loaded with 100 µl 1:10,000 dilution of Pab_{pep}-*Pgl*PGIP1 in dilution buffer (PBS containing 0.1 % BSA) and incubated for 1 h at 37 °C. After washing, the second antibody goat anti-rabbit IgG conjugated with HRP (Bangalore Genei) was added at a dilution of 1:20,000 in dilution buffer and incubated for 1 h at 37 °C. The conjugated enzyme was detected by addition of the substrate *o*-phenylenediamine at 0.04 % (100 µl $well^{-1}$) in PBS containing 0.02 % H_2O_2. The reaction was incubated at room temperature for 10 min and stopped by adding 10 µl of 1 M H_2SO_4. The colorimetric absorbance values were recorded at 490 nm using a microtiter plate reader (SpectraMax® 340PC 384, Molecular Devices Corporation, USA).

Total RNA isolation and cDNA preparation

Total RNA was extracted from 2-day-old IP18296 and 7042S (control and inoculated) samples harvested at 0, 6, 12, 24 and 48 h.p.i. using Total Plant RNA Isolation Kit (Sigma) as per the manufacturer's protocol. Eluted RNA was stored at −80 °C and then treated with DNase I (RNase free) (Fermentas). cDNA was synthesized in 25 µl reactions containing 2 µg of RNA, 0.5 µg of oligo$(dT)_{18}$ primer and 20 units of RiboLock RNase Inhibitor at 42 °C with 0.2 unit of RevertAid M-MuLV Reverse Transcriptase (Fermentas) for 1 h.

Expression analyses of *Pglpgip1* in IP18296 and 7042S seedlings by quantitative real-time PCR (qRT-PCR)

Gene-specific primers RT-*pgip*1-forward (5′-GTGCTGT CGCACAACATCCT-3′)/RT-*pgip*1-reverse (5′-CAGGTC GATCTGCGAAAACC-3′) for the target gene *Pglpgip1* (Acc. No.: JF421287) and RT-*gapdh*-forward (5′-GCCC TCCAGAGTGAGGATGTC-3′)/RT-*gapdh*-reverse 5′-GG TCATGTATTCGGTGGTGATG-3′) for the reference gene *Pglgapdh* (Acc. No.: GQ398107) were designed with Primer Express version 3.0 software (Applied Biosystems). qRT-PCR was carried out with the StepOnePlus™ Real-Time PCR Systems (Applied Biosystems, Germany). Reactions were set up in a total volume of 20 µl using 20 ng cDNA, 1× SYBR Green PCR master mix (SYBR Green mix, Applied Biosystems) and 3 pmol of forward and reverse primers. The cycling conditions were: 95 °C for 10 min, 40 cycles of 15 s at 95 °C, 60 s at 60 °C. Fluorescence acquisition was carried out at 60 °C. At the end of each reaction, a melting curve was generated using a single cycle consisting of 15 s at 95 °C and 60 s at 60 °C. This was followed by a slow temperature increase to 95 °C at the rate of 0.3 °C s^{-1}. The relative quantification of target mRNAs used a comparative C_t method [49] with 0 h 7042S uninoculated water-treated control as the positive calibrator. Suitable non-template and template only controls were maintained. Prior to the relative quantification experiments the optimization of primer concentrations and the determination of PCR efficiency between the reference and target samples were carried out separately. In a separate experiment, the primer specificities were evaluated by PCR using recombinant plasmid DNA containing the target (*Pglpgip1*) and the reference (*Pglgapdh*) genes as template. The resulting amplicons were further confirmed by nucleotide sequencing.

Confocal-immunofluorescence microscopy

The tissue was prepared according to the protocol of Préstamo et al. [50] with minor modifications. Control and treated seedlings harvested at 0 h and 24 h.p.i. were fixed in 4 % (w/v) formaldehyde in PBS for 2 h at room temperature. Samples were then washed thrice, 10 min each in PBS. Sections (30 µm thick) were cut on a Vibratome VT1200S (Leica, Germany) and placed onto glutaraldehyde activated, 3-aminopropyltrietoxysilane coated slides.

Sections were permeabilized with 2 % (w/v) cellulase in wash buffer (25 mM Tris–HCl, pH 7.4, 140 mM NaCl, 3 mM KCl) for 30 min at room temperature. After three washes in wash buffer of 5 min each, the sections were blocked with 5 % BSA (w/v) in wash buffer for 30 min. After washing, the blot was incubated for 1 h at room temperature with Pab_{pep}-*Pgl*PGIP1 diluted 1:10,000 in wash buffer. After three washes in wash buffer of 15 min each, the sections were treated for 1 h at room temperature with goat anti-rabbit IgG-Atto488 diluted 1:2,000 in wash buffer. The sections were then washed thrice in wash buffer of 15 min each and observed for fluorescence with excitation (485 nm) and emission (506–538 nm) filters with a LSM-710 laser scanning confocal microscope (Carl Zeiss, Germany). An objective magnification of 20× with a numeric aperture of 1.3 units was employed. Fluorescent images were acquired through a mounted CCD camera and processed using ZEN 2011 software (Carl Zeiss).

Statistical analyses

All experiments were performed twice independently each in triplicates. The data of a representative experiment was subjected to Tukey's honestly significant difference (HSD) test following analysis of variance (ANOVA) at $p < 0.05$.

Results

Production of polyclonal antibody and immunopurification of a pearl millet PGIP

Pab_{pep}-PglPGIP1 was determined to be absolutely specific to pearl millet PGIP1

Pab_{pep}-*Pgl*PGIP1 was specified by the supplier to have a titer of >1:10,000 determined against 10 µg peptide antigen (CQTQLFNVSYNQLCG). Pab_{pep}-*Pgl*PGIP1 at 1:10,000 dilution was used for all future experiments. Immunoblot analysis using Pab_{pep}-*Pgl*PGIP1 showed reaction only against r*Pgl*PGIP1 and pearl millet total protein (Fig. 1). Further, the antibody showed absolutely no reaction against rVC, the total proteins from various monocot and dicot plant species (Fig. 1a) as well as the unrelated proteins (Fig. 1b). In addition, the control experiments involving preimmune serum and the secondary antibody alone showed no reactivity with the r*Pgl*PGIP1/*Pgl*PGIP1 (Supplementary Fig. 1S).

Immunopurification and characterization of PGIP from pearl millet

Total protein from 2-day-old IP18296 seedlings harvested at 24 h.p.i. was purified on a Pab_{pep}-*Pgl*PGIP1-Sepharose 4B affinity matrix with yields of ~10 µg purified protein per kg of pearl millet tissue. Separation of the purified protein by 2D-gel electrophoresis resulted in an intense protein spot observed at ~43 kDa with a pI value of 5.9 (Fig. 2). Further, the 2D protein spot was subjected to trypsin digestion and the resulting peptides were analyzed by MALDI-TOF MS. Mascot PMF search against NCBInr protein database showed identity to the deduced amino acid sequences of *Pglpgip1* (Score 82; 6 peptide matches; Acc. No.: JF421287) and *Pglpgip1p* (Score 60; 4 peptide matches; Acc. No.: GU474543) (Fig. 3). Hence, the purified protein was designated as *Pgl*PGIP1.

Due to limited amounts of the pure protein the deglycosylation studies were carried out using total proteins from 2-day-old IP18296 seedlings harvested at 24 h.p.i. Western blot analysis of the untreated and chemically deglycosylated total proteins using Pab_{pep}-*Pgl*PGIP1 showed a clear shift in the protein mobility (Fig. 4). The untreated lane showed a single protein band at ~43 kDa whereas chemical deglycosylation resulted in a ~35 kDa band.

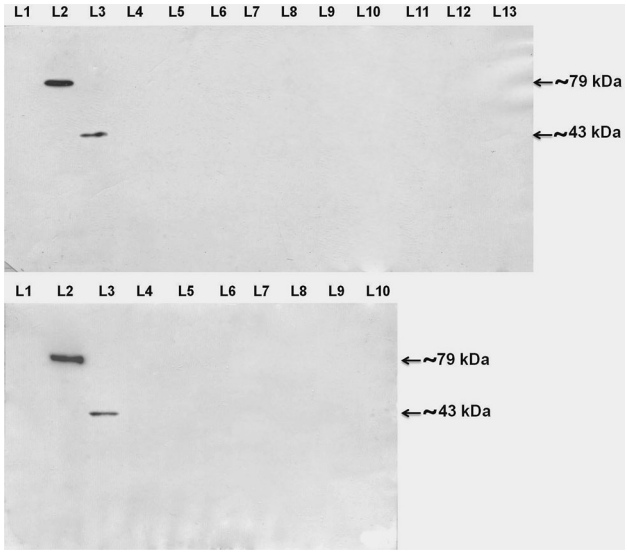

Fig. 1 Immunoblots showing the specificity of Pab_{pep}-*Pgl*PGIP1 for *Pgl*PGIP1. **a** Antibody specificity was assessed by immunoblot analysis against vector control (L1), purified r*Pgl*PGIP1 (L2) (5 µg each) produced in *Escherichia coli* and 50 µg each of crude protein extracts from pearl millet (L3), wheat (L4), rice (L5), sorghum (L6), maize (L7), French bean (L8), tomato (L9), potato (L10), soybean (L11), cotton (L12) and capsicum (L13). **b** Antibody cross reactivity was investigated by including various unrelated proteins such as r*Fm*PGIII (L4), *An*PGII (L5), BSA (L6), myosin (L7), laminarin (L8), RNase A (L9) and DNase I (L10) (2 µg each). Vector control (L1), purified r*Pgl*PGIP1 (L2) (5 µg each) produced in *Escherichia coli* and 50 µg crude protein extract from pearl millet (L3) served as controls. Proteins were separated by SDS-PAGE and blotted onto PVDF membrane. The blot was treated with 1:10,000 dilution of Pab_{pep}-*Pgl*PGIP1 and 1:20,000 diluted secondary antibody; goat anti-rabbit IgG-HRP conjugate. The blot was developed for chemiluminescence signals

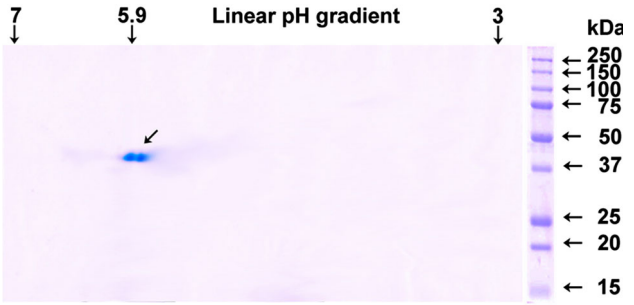

Fig. 2 2D gel showing purified *Pgl*PGIP1. Total protein from IP18292 cultivar was purified on a Pab_{pep}-*Pgl*PGIP1-Sepharose 4B affinity matrix. About 5 µg purified *Pgl*PGIP1 was separated on a 7 cm 3–7 linear IPG strip in the first dimension and SDS-PAGE in the second dimension. The protein spot was visualized by Coomassie Brilliant Blue R-250 staining

PG inhibition studies of *Pgl*PGIP1

PglPGIP1 partially inhibits AnPGII but not rFmPGIII

The in vitro inhibition of purified *Pgl*PGIP1 was carried out against *An*PGII and r*Fm*PGIII in order to compare it with the known inhibition profile of r*Pgl*PGIP1 [42] against the same two PGs. The *Pgl*PGIP1 displayed an activity profile similar to r*Pgl*PGIP1 against the fungal PGs used in the present study, with only a partial inhibition observed against *An*PGII (Fig. 5a) and no inhibition of r*Fm*PGIII. The effect of various parameters on *An*PGII inhibition will be elucidated in the following.

Effect of inhibitor concentration on AnPGII activity

*Pgl*PGIP1 showed marginally higher inhibition of the PG at all tested concentrations compared to r*Pgl*PGIP1 and a positive correlation was observed between the degree of inhibition and inhibitor concentration (Fig. 5a). A meagre 2 % inhibition was observed at the lowest *Pgl*PGIP1 concentration tested with no inhibition observed in case of r*Pgl*PGIP1. A significant increase in inhibition was observed at *Pgl*PGIP1/r*Pgl*PGIP1 concentrations of 0.632, 1.26 and 3.16 nM with inhibition being 8 %/7 %, 19 %/16 % and 29 %/26 %, respectively. Addition of *Pgl*PGIP1/r*Pgl*PGIP1 to the assay mixture at 6.32 and 12.64 nM however showed no further significant increase in inhibition, with just 31 %/27 % and 33 %/28 % inhibition, respectively. PGIP concentrations of 3.16 nM and/or 1.26 nM were used in further studies.

Mode of AnPGII inhibition

*Pgl*PGIP1 and r*Pgl*PGIP1 (1.26 and 3.16 nM each) both displayed non-competitive inhibition of *An*PGII as they were found to decrease the enzymes's maximum velocity (V_{max}) without affecting the Michaelis–Menten constant (K_m) (Table 1). The control protein, rVC (1.26 and 3.16 nM), had no effect on the kinetic parameters of *An*PGII.

pH optima of AnPGII inhibition

The *An*PGII inhibition by *Pgl*PGIP1 and r*Pgl*PGIP1 (3.16 nM each) was tested over a pH range of 3.5–5.0. The pH optimum of inhibition for both inhibitors was found to be between 4.0 and 4.5 (Fig. 5b). No inhibition was observed at pH 3.5 and 5.0 in case of r*Pgl*PGIP1. *Pgl*PGIP1, in contrast, showed significant PG inhibition of 24 % at pH 5.0 and 16 % at pH 3.5.

pH and thermal stability of PglPGIP1

*Pgl*PGIP1 and r*Pgl*PGIP1 (3.16 nM each) were found to be stable over a pH range of 4.0–8.0 (Fig. 5c). At pH 3.0 and 9.0 the inhibition potentials of both inhibitors (*Pgl*PGIP1/r*Pgl*PGIP1) decreased significantly. Both inhibitors showed no inhibition at other tested pH values except for a marginal inhibition of 7 % in case of *Pgl*PGIP1 even at pH 10.0.

A marked difference in the thermal stability of the two inhibitor proteins was observed. *Pgl*PGIP1 (3.16 nM) was found to be equally active from 20 to 70 °C with significant inhibitions of 26 and 20 % recorded at 80 and 90 °C (Fig. 5d). An inhibition of 3 % was observed even at 100 °C. However, r*Pgl*PGIP1 (3.16 nM) was found to be equally active only between 20 and 50 °C. The inhibitory activity dropped marginally to 22 % at 60 °C and significantly at 70 °C and 80 °C to 11 and 3 %, respectively. No inhibition was observed beyond this temperature.

Pearl millet–downy mildew interaction

Sclerospora graminicola-induced higher accumulation of PglPGIP1 is recorded only in the resistant IP18296 cultivar

The temporal accumulation pattern of *Pgl*PGIP1 in cultivars IP18296 and 7042S in response to *S. graminicola* was investigated by western blotting (Fig. 6a) and ELISA (Fig. 6b). Both techniques showed pathogen-induced accumulation of the PGIP only in the incompatible interaction with the most intense levels observed at 24 h.p.i. and 48 h.p.i. A significantly higher constitutive level of the PGIP was observed in IP18296. PGIP levels in 7042S were found to be very low throughout the time points tested.

The downy mildew pathogen induces higher accumulation of Pglpgip1 transcripts in the resistant IP18296 cultivar

The relative temporal expression profile of *Pglpgip1* in cultivars IP18296 and 7042S in response to *S. graminicola* was

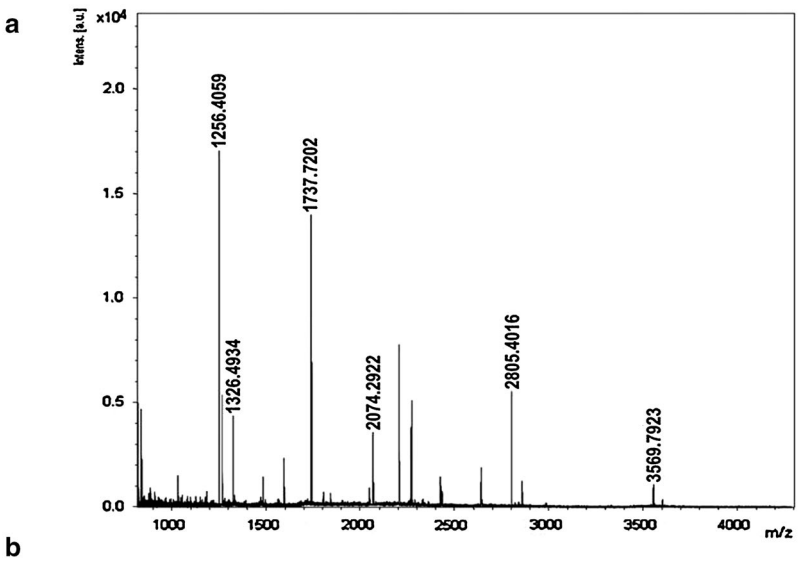

b

MATRIX SCIENCE **Mascot Search Results**

Concise Protein Summary Report

1. gi|375005166 **Mass:** 36228 **Score:** 82 **Expect:** 0.015 **Matches:** 6
polygalacturonase-inhibitor protein 1 [Cenchrus americanus]

Protein sequence coverage: 29% Matched peptides shown in ***bold red***.

```
  1 MSKMKRAMRT MRAILVVLLV AASPAAASPI RCHHDDIAAL AAIGAAFGGY
 51 CSAWTQRDPE CCGGGIHCDP FTGRVTDLAV FQDANITGTI PDAVARLVHL
101 RTLKLHHLPA ISGPIPPAIA KLSNLTMLII SWTGVSGPVP SFLGALTKLT
151 FLDLSFNSLT GVIPASLAAL PNLNGINLSR NRLTGVIPPL LFSKSPDQAS
201 LVLSHNILNG SIPAEFSAVG FSQIDLSRNA FTGDASALFG RGKELQILDL
251 SRNAFSFNLS DVELPERLTW LDLSHNAIYG GIPAQVANMS FQTQLFNVSY
301 NQLCGAVPTG GIMGKFDAYS FQHNKCLCGA PLANLCK
```

Start - End	Observed	Mr(expt)	Mr(calc)	Delta	M	Peptide
102 - 121	2074.2922	2073.2849	2073.2462	0.0387	1	R.TLKLHHLPAISGPIPPAIAK.L
195 - 228	3569.7923	3568.7850	3568.8162	-0.0311	0	K.SPDQASLVLSHNILNGSIPAEFSAVGFSQIDLSR.N
229 - 241	1326.4934	1325.4861	1325.6364	-0.1503	0	R.NAFTGDASALFGR.G
244 - 267	2805.4016	2804.3943	2804.4344	-0.0401	1	K.ELQILDLSRNAFSFNLSDVELPER.L
253 - 267	1737.7202	1736.7129	1736.8369	-0.1240	0	R.NAFSFNLSDVELPER.L
316 - 325	1256.4059	1255.3986	1255.5622	-0.1636	0	K.FDAYSFQHNK.C

gi|300808112 **Mass:** 14466 **Score:** 60 **Expect:** 2.4 **Matches:** 4
polygalacturonase-inhibitor protein [Cenchrus americanus]

Protein sequence coverage: 52% Matched peptides shown in ***bold red***.

```
  1 LDLSFNSLTG VIPASLAALP NLNGINLSRN RLTGVIPPLL FSKSPDQASL
 51 VLSHNILNGS IPAEFSAVGF SQIDLSRNAF TGDASALFGR GKELQILDLS
101 RNAFSFNLSD VELPERLTWL DLSHNAIYGG IPAQVA
```

Start - End	Observed	Mr(expt)	Mr(calc)	Delta	M	Peptide
44 - 77	3569.7923	3568.7850	3568.8162	-0.0311	0	K.SPDQASLVLSHNILNGSIPAEFSAVGFSQIDLSR.N
78 - 90	1326.4934	1325.4861	1325.6364	-0.1503	0	R.NAFTGDASALFGR.G
93 - 116	2805.4016	2804.3943	2804.4344	-0.0401	1	K.ELQILDLSRNAFSFNLSDVELPER.L
102 - 116	1737.7202	1736.7129	1736.8369	-0.1240	0	R.NAFSFNLSDVELPER.L

Fig. 3 Mass spectrometry-based protein identification. **a** MALDI-TOF mass spectrum of trypsin digest of immunopurified pearl millet protein. Total protein from 2-day-old IP18296 seedlings harvested at 24 h.p.i. was purified on a Pab_{pep}-*Pgl*PGIP1-Sepharose 4B affinity matrix. Purified protein was subjected to 2D gel electrophoresis. The resulting protein spot (~43 kDa) was subjected to trypsin digestion and the resulting peptides were analyzed by MALDI-TOF mass spectrometry. The ions showing match to pearl millet PGIP1 have been mentioned in the spectrum. **b** Mascot search results. Mascot PMF search against the NCBInr protein database showed identity to the deduced amino acid sequence of only *Pglpgip1* (Acc. No.: JF421287; GU474543). Peptide matches are shown in *bold red*. (Color figure online)

investigated by qRT-PCR. A basal ~tenfold higher transcript level was observed in IP18292 compared to 7042S (Fig. 7). Pathogen-induced increase in accumulation of *Pglpgip1* transcripts was detected only in IP18292. IP18292 displayed a steady increase in mRNA accumulation which peaked at 24 h.p.i. (71.7-fold over the positive calibrator), and significant levels were found at 12 h.p.i. (33-fold over the positive calibrator) and 48 h.p.i. (45.5-fold over the positive calibrator). The marked difference in *Pglpgip1* expression levels between the highly resistant (IP18296) and highly susceptible (7042S) pearl millet cultivars in response to the downy mildew pathogen indicates a role for this PGIP in host defense.

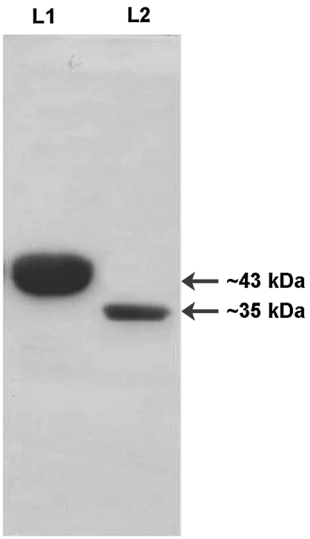

Fig. 4 Immunoblot showing the effect of chemical deglycosylation on *Pgl*PGIP1 mobility. Total protein (50 µg) from IP18292 seedlings was chemically deglycosylated with TFMS. The untreated (L1) and chemically deglycosylated (L2) total proteins (50 µg each) were separated on a 12 % SDS-PAGE gel and blotted onto PVDF membrane. The blot was treated with a 1:10,000 dilution of Pab_{pep}-*Pgl*PGIP1 and 1:20,000 diluted secondary antibody; goat anti-rabbit IgG-HRP conjugate. The blot was developed for chemiluminescence signals

Epidermis and vasculature of IP18296 cultivar showed the most intense accumulation of PglPGIP1 in response to the pathogen

Confocal immuno-fluorescence laser scanning microscopy of coleoptile cross sections of 2-day-old IP18296 and 7042S harvested at 0 and 24 h.p.i. was carried out to understand the tissue localization pattern of *Pgl*PGIP1. Pab_{pep}-*Pgl*PGIP1-treated cross sections of pathogen-inoculated IP18296 seedlings showed higher accumulation of the PGIP over the control (Fig. 8a–c). The pathogen-inoculated IP18296 sample showed a very intense immunodecoration across the coleoptile cross section with highest fluorescence intensities observed at the outer epidermal layer and vascular bundles (Fig. 8c). In contrast, susceptible samples showed very poor signals only in the outer epidermal region (Fig. 8d–f). No major differences were observed in the signal intensities of the corresponding 0 and 24 h control samples in both cultivars. Treatment with pre-immune serum and secondary antibody alone resulted in no signals (data not shown). No significant auto-fluorescence was observed.

Discussion

Purification of PGIPs from various plant sources generally involved the use of size exclusion, ion-exchange, and affinity-based strategies such as Concanavalin-A and PG tagged to Sepharose 4B [15]. Our earlier attempts to purify PGIP/s from pearl millet using size exclusion and ion-exchange matrices were not completely successful [41]. Hence, a PGIP-encoding gene from pearl millet (*Pglpgip1*) was isolated and expressed in *E. coli* to produce recombinant PGIP (r*Pgl*PGIP1) [42]. r*Pgl*PGIP1, assayed against the two fungal PGs, *An*PGII and r*Fm*PGIII, showed partial inhibition of *An*PGII and no inhibition against r*Fm*PGIII [42]. Protein glycosylation is known to be crucial in the acquisition of native protein conformations [51]. Therefore, lack of optimal folding of the recombinant PGIP due to the non-glycosylated nature of the proteins expressed in the bacterial system was construed as a possible explanation for the inhibition behavior. However, such partial inhibitions of PGs have not been unheard of and have been reported in several PG:PGIP systems [15, 30]. Antigen capture using antibody-tagged columns is still popular and being successfully used in purifying numerous proteins in a single step [52, 53]. Hence, a polyclonal antibody, Pab_{pep}-*Pgl*PGIP1, was generated commercially against a highly immunogenic pearl millet PGIP peptide based on the deduced amino acid sequence of *Pglpgip1*, in order to immuno-capture the native *Pgl*PGIP1. Pab_{pep}-*Pgl*PGIP1 was found to interact with purified r*Pgl*PGIP1 (produced in *E. coli*) with absolute specificity. Immunoaffinity purification and mass spectrometry-based protein identity analysis, as expected, resulted in the successful isolation of native *Pgl*PGIP1. Our earlier study had reported the isolation of two partial *pgip* sequences from pearl millet—*Pglpgip1p* (Acc. No.: GU474543) and *Pglpgip2p* (Acc. No.: JQ425039). Further, the study was successful in the isolation of only the complete coding sequence of *Pglpgip1* (Acc. No.: JF421287) by inverse PCR using primers based on *Pglpgip1p* sequence [42]. The PMF analysis showed peptide matches to the deduced amino acid sequences of only *Pglpgip1* and *Pglpgip1p*, and not to *Pglpgip2p*. Hence, the protein immunopurified using total pearl millet extract was assigned as *Pgl*PGIP1. Chemical deglycosylation followed by a protein mobility shift analysis confirmed the protein to be a glycoprotein, which is in line with our earlier report of seven putative *N*-glycosylation sites identified using bioinformatic analysis of *Pglpgip1* [42]. Further, glycan analysis and experimental mapping would be needed to establish the degree and nature of the glycosylation. The purification yields obtained in the present study were rather poor as shown in the results. This is consistent with earlier literature which reports monocots to possess only small amounts of pectin in their CWs [54]. It was reported that, just 350 ng of PGIP could be isolated per gram of wheat leaf tissue and wheat PGIP levels were found to be 60 times lower (approximately 0.000035 % (w/w) from fresh wheat leaves) than those observed in pear [30].

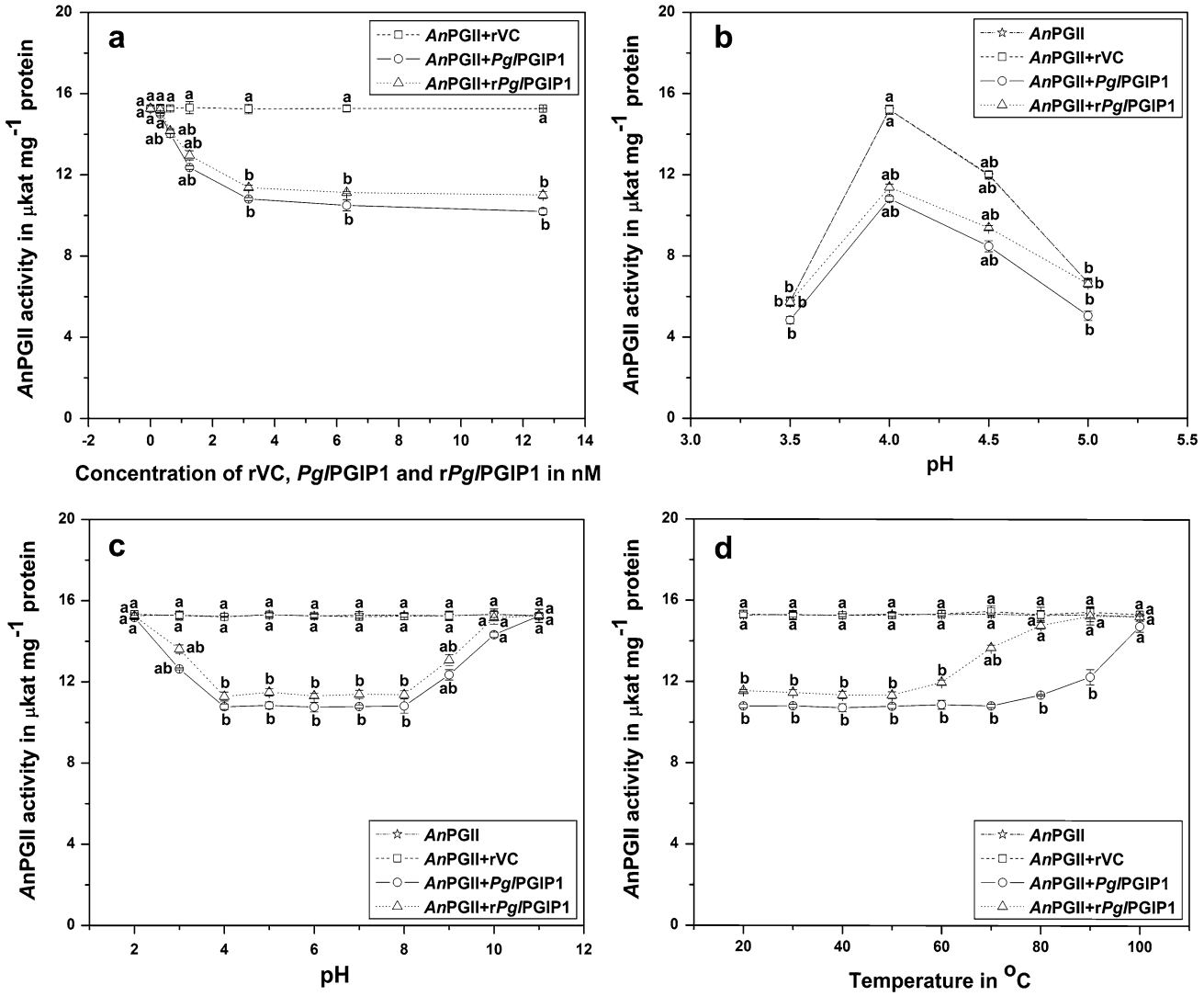

Fig. 5 *An*PGII inhibition assay. **a** Effect of inhibitor concentration. *An*PGII (5 ng) was assayed with and without inhibitor (*Pgl*PGIP1/r*Pgl*PGIP1) and control protein (rVC), over a concentration range of 0.316–12.64 nM and a plot representing the enzyme activity over inhibitor concentration was generated. **b** pH optimum. *An*PGII (5 ng) was assayed with and without inhibitor (*Pgl*PGIP1/r*Pgl*PGIP1) and control protein (rVC), at a concentration of 3.16 nM and a plot representing the enzyme activity over pH units was generated to determine the pH optima of inhibition. **c** pH stability. *An*PGII (5 ng) was assayed with and without inhibitor (*Pgl*PGIP1/r*Pgl*PGIP1) and control protein (rVC), pre-incubated for 16 h at pH values 2.0–10.0, at 4 °C upon reconstitution in the assay buffer at a concentration of 3.16 nM and a plot representing the enzyme activity over pH units was generated to determine the pH stability of inhibitor. **d** Temperature stability. *An*PGII (5 ng) was assayed with and without inhibitor (*Pgl*PGIP1/r*Pgl*PGIP1) and control protein (rVC), pre-incubated for 1 h at temperatures ranging from 20 to 100 °C at a concentration of 3.16 nM and a plot representing the enzyme activity over temperature was generated to determine the temperature stability of inhibitor. The data points are means of a single experiment carried out in triplicates. *Bars* indicate ± standard error. Means designated with the same letter are not significantly different according to Tukey's HSD test at $p < 0.05$

The glycoproteinaceous nature of plant PGIPs has been confirmed by chemical and enzymatic deglycosylation studies [55–57]. The degree of glycosylation is known to vary with the plant species [56]. Bergmann et al. [58] proposed the glycan component of the glycoproteins to be of importance in binding and recognition of PGs and proposed a possible association between the extent of PGIP glycosylation and its inhibition specificity. The protein model of pear PGIP with the most abundant glycan structures revealed the N-linked glycans to lie on both sides of the binding surface. This was shown to greatly increase both available surface area and potential for steric modulation of target PG binding [59]. However, this model needs experimental verification and since then not much effort has gone into understanding the effect of carbohydrate moieties on PG inhibition. Hence, the non-

Table 1 The kinetic parameters of *An*PGII with and without *Pgl*PGIP1/r*Pgl*PGIP1/rVC

	V_{max} (μkat mg^{-1} protein)	K_m (mg ml^{-1})
*An*PGII	28.8	0.094
*An*PGII + rVC (1.26 nM)	28.8	0.093
*An*PGII + rVC (3.16 nM)	28.9	0.094
*An*PGII + *Pgl*PGIP1 (1.26 nM)	23.3	0.094
*An*PGII + *Pgl*PGIP1 (3.16 nM)	20.5	0.094
*An*PGII + r*Pgl*PGIP1 (1.26 nM)	24.4	0.093
*An*PGII + r*Pgl*PGIP1 (3.16 nM)	21.5	0.094

*An*PGII (5 ng) was assayed using a substrate concentration range of 0.025–0.25 mg/ml with and without inhibitors (*Pgl*PGIP1/r*Pgl*PGIP1) and control protein (rVC), each at concentrations of 1.26 and 3.16 nM. The kinetic parameters were calculated by fitting the Michaelis–Menten equation on initial rate experimental data by non-linear fitting using OriginPro 7 (Originlab)

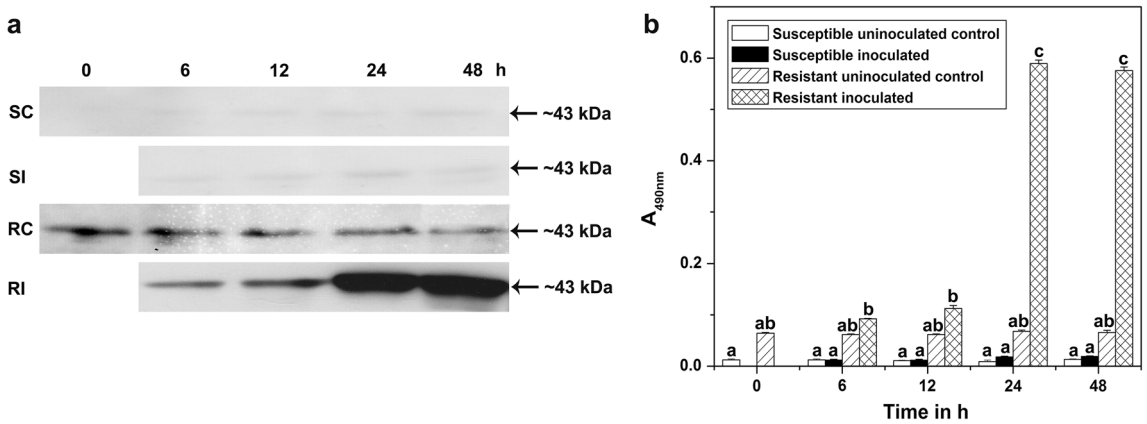

Fig. 6 Temporal accumulation levels of *Pgl*PGIP1 in 2-day-old IP18292 and 852B pearl millet seedlings in response to pathogen inoculation. **a** Western blot analysis. Total pearl millet protein (50 μg) from different samples i.e., resistant (IP18292) uninoculated control (RC), resistant (IP18292) pathogen-inoculated (RI), susceptible (7042S) uninoculated control (SC), and susceptible (7042S) pathogen-inoculated (SI) pearl millet seedlings harvested at 0, 6, 12, 24 and 48 h.p.i. were separated by SDS-PAGE and electro-blotted onto a PVDF membrane. The blot was treated with a 1:10,000 dilution of Pab_{pep}-*Pgl*PGIP1 and 1:20,000 diluted secondary antibody; goat anti-rabbit IgG-HRP conjugate. The blot was developed for chemiluminescence signals. **b** ELISA analysis. The accumulation of *Pgl*PGIP1 in the same set of samples used for immunoblot analysis was also studied by ELISA using Pab_{pep}-*Pgl*PGIP1 (primary antibody; 1:10,000 dilution) and goat anti-rabbit IgG conjugated with HRP (secondary antibody; 1:20,000 dilution). The conjugated enzyme was colorimetrically assayed at 490 nm using a microtiter plate reader. Values are means of a single experiment carried out in triplicates. The *bars* indicate ± standard error. Means designated with the *same letter* are not significantly different according to Tukey's HSD test at $p < 0.05$

glycosylated (r*Pgl*PGIP1) and the native glycosylated (*Pgl*PGIP1) PGIPs were assayed for inhibition against *An*PGII and r*Fm*PGIII to resolve the role of glycosylation on PG:PGIP interaction. The comparative inhibition studies showed both PGIP forms to be similar in their behavior against the two fungal PGs tested. There was no significant difference in the extent and mode of *An*PGII inhibition by both inhibitors. However, the native form was found to be more stable to changes in pH and temperature, which could be due to the glycosylation. Glycosylation has been reported to lead to increased stability against variations in the physico-chemical environment of the protein such as precipitation, pH, chemical and thermal denaturation, and aggregation [60]. The functionality of the native *Pgl*PGIP1 over a wider range of pH units could be crucial when countering varied pathogen PGs under diverse environments and in the generation of OG-elicitors leading to a better host defense [61]. The results obtained in the present study indicate that the mere glycosylation of PGIP does not impart it with an ability to inhibit a PG (r*Fm*PGII in this case); but the glycans can improve the physico-chemical stability of the PGIP. However, extensive studies involving multiple PG:PGIP systems are necessary before coming to such generalized conclusions.

An earlier study using probes generated against bean PGIP in pearl millet-downy mildew interaction did indicate

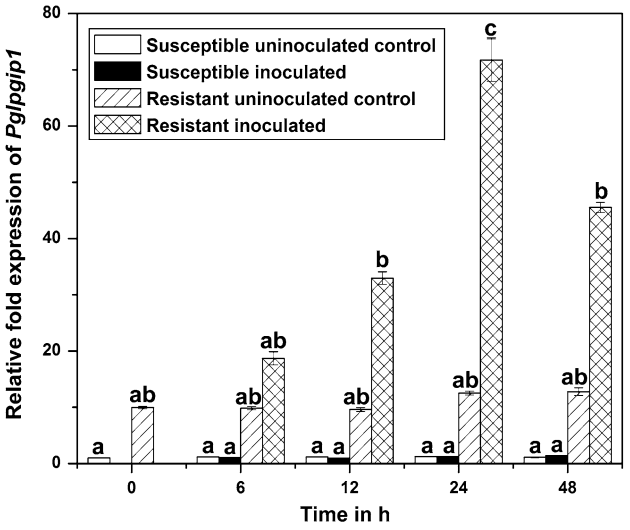

Fig. 7 Relative expression levels of the *Pglpgip1* transcript in 2-day-old IP18292 and 7042S seedlings in response to pathogen inoculation. Expression levels of the target gene *Pglpgip1* were measured in 2-day-old IP18292 (resistant) and 7042S (susceptible) seedlings (harvested at 0, 6, 12, 24 and 48 h.p.i.) by qRT-PCR and normalized to the constitutive reference gene *Pglgapdh*. The relative quantification of target transcripts used a comparative C_t method with a 0 h 7042S uninoculated water-treated control as the positive calibrator. Values are means of a single experiment carried out in triplicates. The *bars* indicate ± standard error. Means designated with the *same letter* are not significantly different according to Tukey's HSD test at $p < 0.05$

a role for the inhibitor protein in host resistance [40]. However, the identity of the reactive transcript and proteins could not be verified. Therefore, the present study was carried out with native biomolecular tools to reassess and confirm the role of PGIP in host resistance against *S. graminicola*.

The role of PGIP in the present host-pathogen system was appraised by comparative temporal changes in accumulation of protein and transcripts between resistant and susceptible pearl millet cultivars challenged with the oomycetous pathogen. Results show a clear differential accumulation of *Pgl*PGIP1 as well as its encoding transcript between compatible and incompatible interactions. Only the resistant cultivar showed a strong constitutive *pgip* expression as well as pathogen-induced higher accumulation. Unlike differential transcript accumulation at 24 and 48 h.p.i. in case of the resistant sample, protein fortification was found to be similar at both these time points. This indicates that high PGIP levels are retained even at later stages to counter the pathogen ingress without necessary increase in transcript levels. Glycosylation has been reported to protect proteins against proteolytic degradation and thus increasing their retention times which could be the case here, too [60]. Observation of very poor accumulation of PGIP in compatible interaction clearly points towards the significance of PGIP in pearl millet-downy mildew interaction. Similar studies in various plants have demonstrated the importance of PGIPs in plant-pathogen interaction. In potato-*Phytophthora infestans*, Japanese pear-*Venturia nashicola*, Dutch elm-*Ophiostoma novoulmi* and pea-*Heterodera goettingiana* interactions differential higher accumulation of *pgip* transcripts and their encoded proteins were observed only in the disease resistant cultivar [57, 62–64]. An extensive qRT-PCR analysis of the *pgip* gene family upon inoculation of bean with three different fungi such as *B. cinerea*, *Colletotrichum lindemuthianum* and *Sclerotinia sclerotiorum* showed significant increase in the transcript levels of *Pvpgip1-3* with the *Pvpgip2* levels being the highest. In addition, an early induction of *Pvpgip1-3* was observed in bean-*C. lindemuthianum* incompatible interaction with a late accumulation of the genes observed in the compatible interaction [65].

PGIP was shown to be part of an early defense in tomato-*Orobanche ramosa* interaction and grapevine treated with *B. cinerea*, with transcript upregulation recorded as early as 1–2 and 6 h.p.i. [66, 67]. However, in soybean-*S. sclerotiorum*, poplar-*Marssonina brunnea* f. sp. *multigermtubi* and rice-*Rhizoctonia solani* interactions late accumulation of the *pgip* transcripts varying between 24 and 96 h.p.i. has been observed [17, 31, 68]. The relatively late accumulation of PGIPs in pearl millet could be due to strong constitutive levels observed in the resistant cultivar possibly sufficient to defy very low levels of PG secreted by biotrophic pathogens during initial infection phase. This is further supported by the lack of detectible PG activity in infected pearl millet. Similarly, in pea, PGIP expression was upregulated in response to the cyst nematode invasion even though no PG activity was detected [64]. Though *endo*-PGs are known to be the first enzymes secreted by necrotrophic phytopathogens for plant penetration [69], obligate pathogens are known to typically secrete limited amounts of PGs and other lytic enzymes to evade host detection through extensive tissue damage [70, 71].

Though pearl millet roots and coleoptiles are available for infection by *S. graminicola*, most pathogen propagules are localized in the mesocotyl and shoot regions of the seedlings [72]. This together with no detectable PGIP signals in case of the pearl millet root fraction during immunoblot analysis (results not shown) prompted us to choose coleoptile sections for in situ PGIP localization studies. Confocal immuno-staining results of PGIP in 0 and 24 h.p.i. samples were consistent with the earlier protein accumulation studies at these times. The PGIP was localized to very high levels mostly in the epidermal and vascular bundle tissues, with less intense accumulation in the parenchyma beneath. Organ-specific (young leaves, hypocotyls, roots and pods) accumulation studies of *pgip* transcript in bean showed a differential expression of the *pgip*

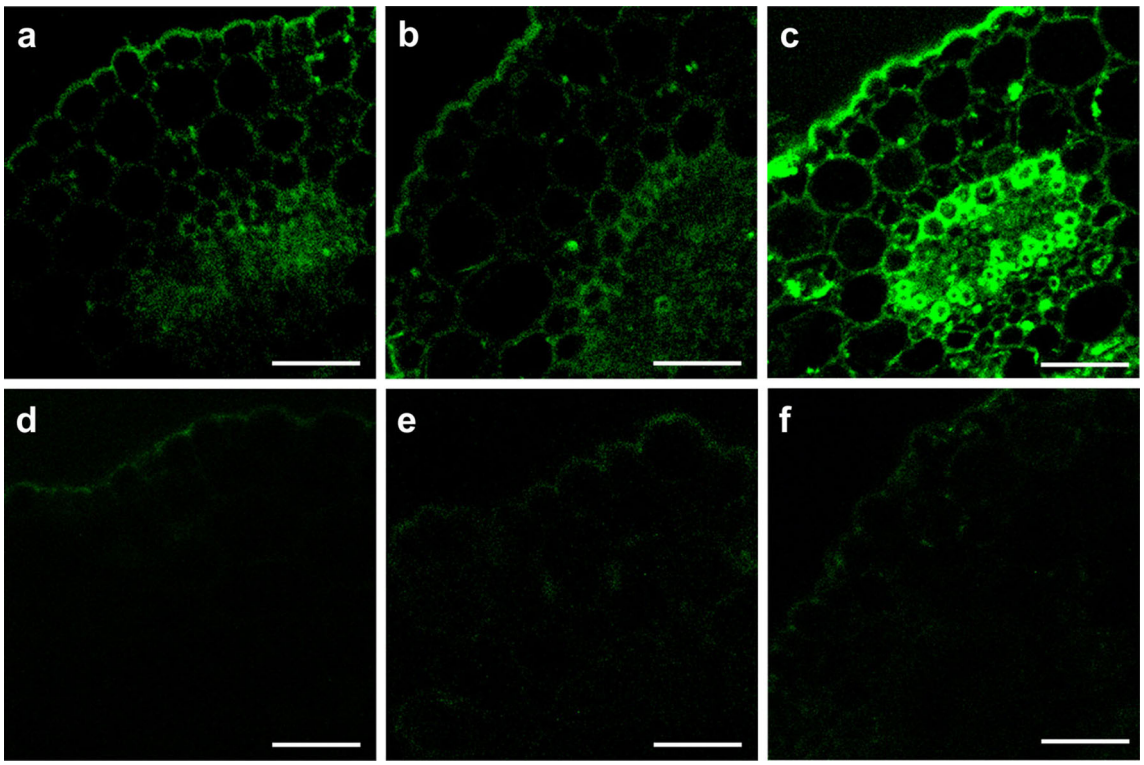

Fig. 8 Immuno-histochemical localization of *Pgl*PGIP1 in 2-day-old IP18292 and 7042S seedlings in response to pathogen inoculation. Vibratome coleoptile sections (30 μm thick) of 2-day-old IP18292 (resistant) and 7042S (susceptible) seedlings harvested at h and 24 h.p.i. were treated with 1:5,000 dilution of Pab_{pep}-*Pgl*PGIP1. The fluorescence detection of bound primary antibody under a LSM-710 laser scanning confocal microscope was achieved by using a 1:10,000 dilution of secondary antibody, anti-rabbit IgG-Atto488 whole molecule produced in goat. The samples include: **a** resistant uninoculated control, 0 h; **b** resistant uninoculated control, 24 h; **c** resistant pathogen-inoculated, 24 h.p.i.; **d** susceptible uninoculated control, 0 h; **e** susceptible uninoculated control, 24 h; and **f** susceptible pathogen-inoculated, 24 h.p.i. pearl millet seedlings. *Bar* = 50 μm

gene family. The *Pvpgip2* was expressed in all organs, *Pvpgip1* in none and *Pvpgip3-4* expressed poorly in roots [65]. In the bean-*C. lindemuthianum* incompatible interaction, in situ experiments showed a rapid, intense and transient accumulation of *pgip* mRNA in epidermal cells proximal to the site of infection and, less intense, within the cortical parenchyma underneath [73]. In compatible interactions, no significant accumulation was observed in hypocotyls and a very weak accumulation seen in leaves during lesion formation [74]. Immuno-localization of wheat PGIP also showed it to be present in CWs of epidermal and cortical parenchymal cells [30]. Immuno-localization of PGIP in leaves, stems and roots of *Chorispora bungeana* showed even distribution in leaves, mainly localized in epidermis, and in vascular bundles in stems and roots. The fluorescence signal of the control was nearly absent in stem, but not in leaf and root [75]. Protein trafficking studies in tobacco showed a bean PGIP2-green fluorescent protein fusion to move as a soluble cargo protein along the secretory pathway before internalization into the vacuole. CW localization of this protein occurred only upon its encounter of a specific fungal PG [76]. Recently wheat *pgip*s were shown to be active at the site of the lesion caused by pathogen infection [27]. Such spatially regulated activation of PGIP expression during infection therefore suggests a role for PGIP in pearl millet defense response. However, the constitutive levels of the PGIP in pearl millet also hints at a possible role for the protein in either developmental processes or in cellular mechanisms associated with host defense such as CW modulation. This is corroborated by earlier studies which have shown *pgip* to be involved in processes such as regulation of floral organ development in rice [26], petal development and senescence in cotton [77], pollen development in Chinese cabbage-pak-choi [78] and seed germination in *Arabidopsis* [79].

In conclusion, using comparative PG inhibition analyses involving the native, immunopurified PGIP from pearl millet and its non-glycosylated recombinant form, the present study has shown the glycan component to influence the pH and thermal stabilities of *Pgl*PGIP1. Further, differential spatio-temporal accumulation of *Pgl*PGIP1 between the compatible and incompatible interactions shows a role for the protein in pearl millet's defense against

the downy mildew pathogen. However, transgenic over-expression and knock-out of *Pglpgip*1 and assessment of its expression levels on disease incidence and plant morphology and physiology would prove its involvement in host resistance and/or development beyond doubt. In addition, isolation and characterization of all pearl millet *pgip*s would be crucial for a comprehensive understanding of the full impact of the gene family on plant defense and development. This could further be exploited in devising pearl millet cultivars with better growth characteristics and resistance to pathogens.

Acknowledgments The first author is thankful to the Department of Biotechnology, Government of India, European Molecular Biology Organization, Germany and Prof. Dr. Bruno Moerschbacher, Institut für Biologie und Biotechnologie der Pflanzen, Westfälische Wilhelms-Universität Münster, Germany for the financial support in the form of fellowships. We thank Mr. Madhusudhan, University of Mysore, Mysore, India and Prof. Francesco Favaron, Dip. Territorio e Sistemi agro-forestali, sez. Patologia Vegetale, Universita degli Studi di Padova, Viale dell_Universita 16, I-35020 Legnaro, Italy for purified *An*PGII and *Fm*PGIII clone, respectively. We also acknowledge the recognition of University of Mysore as an Institution of Excellence by the Government of India with financial support from the Ministry of Human Resource Development and University Grants Commission, India.

References

1. Bashline L, Lei L, Li S, Gu Y (2014) Cell wall, cytoskeleton, and cell expansion in higher plants. Mol Plant. doi:10.1093/mp/ssu018
2. Keegstra K (2010) Plant cell walls. Plant Physiol 154:483–486
3. Vorwerk S, Somerville S, Somerville C (2004) The role of plant cell wall polysaccharide composition in disease resistance. Trends Plant Sci 9:203–209
4. Karr A, Albersheim P (1970) Polysaccharide-degrading enzymes are unable to attack plant cell walls without prior action by a "wall-modifying enzyme". Plant Physiol 46:69–80
5. Douaiher M, Nowak E, Durand R et al (2007) Correlative analysis of *Mycosphaerella graminicola* pathogenicity and cell wall-degrading enzymes produced in vitro: the importance of xylanase and polygalacturonase. Plant Pathol 56:79–86
6. Roper M, Greve L, Warren J et al (2007) *Xylella fastidiosa* requires polygalacturonase for colonization and pathogenicity in *Vitis vinifera* grapevines. Mol Plant Microbe Interact 20:411–419
7. Jaroszuk-Scisel J, Kurek E, Słomka A et al (2011) Activities of cell wall degrading enzymes in autolyzing cultures of three *Fusarium culmorum* isolates: growth-promoting, deleterious and pathogenic to rye (*Secale cereale*). Mycologia 103:929–945
8. Jia Y, Feng B, Sun W, Zhang X (2009) Polygalacturonase, pectate lyase and pectin methylesterase activity in pathogenic strains of *Phytophthora capsici* incubated under different conditions. J Phytopathol 157:585–591
9. Sun W, Jia Y, Feng B et al (2009) Functional analysis of Pcipg2 from the straminopilous plant pathogen *Phytophthora capsici*. Genesis 47:535–544
10. De Lorenzo G, D'Ovidio R, Cervone F (2001) The role of polygalacturonase-inhibiting proteins (PGIPs) in defense against pathogenic fungi. Annu Rev Phytopathol 39:313–335
11. Federici L, Di Matteo A, Fernandez-Recio J et al (2006) Polygalacturonase inhibiting proteins: players in plant innate immunity? Trends Plant Sci 11:65–70
12. D'Ovidio R, Raiola A, Capodicasa C et al (2004) Characterization of the complex locus of bean encoding polygalacturonase-inhibiting proteins reveals sub-functionalization for defense against fungi and insects. Plant Physiol 135:2424–2435
13. Schacht T, Unger C, Pich A, Wydra K (2011) Endo- and exo-polygalacturonases of *Ralstonia solanacearum* are inhibited by polygalacturonase-inhibiting protein (PGIP) activity in tomato stem extracts. Plant Physiol Biochem 49:377–387
14. Cervone F, De Lorenzo G, Pressey R et al (1990) Can phaseolus PGIP inhibit pectic enzymes from microbes and plants? Phytochemistry 29:447–449
15. Gomathi V, Gnanamanickam S (2004) Polygalacturonase-inhibiting proteins in plant defence. Curr Sci 87:1211–1217
16. Misas-Villamil J, Van der Hoorn R (2008) Enzyme-inhibitor interactions at the plant-pathogen interface. Curr Opin Plant Biol 11:380–388
17. Cheng Q, Cao Y, Pan H et al (2008) Isolation and characterization of two genes encoding polygalacturonase-inhibiting protein from *Populus deltoids*. J Genet Genomics 35:631–638
18. Shivashanker S, Thimmareddy C, Roy T (2010) Polygalacturonase inhibitor protein from anthracnose resistant and susceptible varieties of Chilli (*Capsicum annuum* L.). Indian J Biochem Biophys 47:243–248
19. D'Ovidio R, Mattei B, Roberti S, Bellincampi D (2004) Polygalacturonases, polygalacturonase-inhibiting proteins and pectic oligomers in plant-pathogen interactions. Biochim Biophys Acta 1696:237–244
20. Powell A, Van Kan J, Ten Have A et al (2000) Transgenic expression of pear PGIP in tomato limits fungal colonization. Mol Plant Microbe Interact 13:942–950
21. Manfredini C, Sicilia F, Ferrari S et al (2005) Polygalacturonase-inhibiting protein 2 of *Phaseolus vulgaris* inhibits BcPG1, a polygalacturonase of *Botrytis cinerea* important for pathogenicity, and protects transgenic plants from infection. Physiol Mol Plant Pathol 67:108–115
22. Hwang B, Bae H, Lim H-S et al (2010) Overexpression of polygalacturonase-inhibiting protein 2 (PGIP2) of Chinese cabbage (*Brassica rapa* ssp. pekinensis) increased resistance to the bacterial pathogen *Pectobacterium carotovorum* ssp. carotovorum. Plant Cell Tissue Organ Cult 103:293–305
23. Perez-Donoso A, Sun Q, Roper M et al (2010) Cell wall-degrading enzymes enlarge the pore size of inter-vessel pit membranes in healthy and *Xylella fastidiosa*-infected grapevines. Plant Physiol 152:1748–1759
24. Ferrari S, Sella L, Janni M et al (2011) Transgenic expression of polygalacturonase-inhibiting proteins in Arabidopsis and wheat increases resistance to the flower pathogen *Fusarium graminearum*. Plant Biol 14:31–38
25. Ferrari S, Galletti R, Vairo D et al (2006) Antisense expression of the *Arabidopsis thaliana* AtPGIP1 gene reduces polygalacturonase-inhibiting protein accumulation and enhances susceptibility to *Botrytis cinerea*. Mol Plant Microbe Interact 19:931–936
26. Jang S, Lee B, Kim C, Kim S et al (2003) The OsFOR1 gene encodes a polygalacturonase inhibitory protein (PGIP) that regulates floral organ number in rice. Plant Mol Biol 53:357–369
27. Janni M, Bozzini T, Moscetti I et al (2013) Functional characterisation of wheat Pgip genes reveals their involvement in the local response to wounding. Plant Biol 15:1019–1024
28. Janni M, Di Giovanni M, Roberti S et al (2006) Characterization of expressed Pgip genes in rice and wheat reveals similar extent of sequence variation to dicot PGIPs and identifies an active PGIP lacking an entire LRR repeat. Theor Appl Genet 113:1233–1245

29. Janni M, Sella L, Favaron F et al (2008) The expression of a bean PGIP in transgenic wheat confers increased resistance to the fungal pathogen *Bipolaris sorokiniana*. Mol Plant Microbe Interact 21:171–177
30. Kemp G, Bergmann C, Clay R et al (2003) Isolation of a polygalacturonase-inhibiting protein (PGIP) from wheat. Mol Plant Microbe Interact 16:955–961
31. Lu L, Zhou F, Zhou Y et al (2012) Expression profile analysis of the polygalacturonase-inhibiting protein genes in rice and their responses to phytohormones and fungal infection. Plant Cell Rep 31:1173–1187
32. Rajaram E, Nepolean T, Senthilvel S et al (2013) Pearl millet [*Pennisetum glaucum* (L.) R. Br.] consensus linkage map constructed using four RIL mapping populations and newly developed EST-SSRs. BMC Genome 14:159
33. Sehgal D, Rajaram V, Vadez V et al (2012) Integration of gene based markers in pearl millet genetic map for identification of candidate genes underlying drought tolerance quantitative trait loci. BMC Plant Biol 12:9
34. Thakur R, Rai K, Khairwal I, Mahala R (2008) Strategy for downy mildew resistance breeding in pearl millet in India. J SAT Agric Res 6:1–11
35. Shailasree S, Kini R, Shetty H (2007) Beta-amino butyric acid-induced resistance in pearl millet to downy mildew is associated with accumulation of defense-related proteins. Australas Plant Pathol 36:204–211
36. Raj S, Chaluvaraju G, Amruthesh K, Shetty H (2004) Induction of growth promotion and resistance against downy mildew on pearl millet (*Pennisetum glaucum*) by rhizobacteria. Plant Dis 87:380–384
37. Hash C, Sharma A, Kolesnikova-Allen M et al (2006) Teamwork delivers biotechnology products to Indian small-holder crop-livestock producers: pearl millet hybrid "HHB 67 Improved" enters seed delivery pipeline. J SAT Agric Res 2:16–20
38. Raminenei R, Sadumpati V, Khareedu V, Vudem D (2014) Transgenic pearl millet male fertility restorer line (ICMP451) and hybrid (ICMH451) expressing *Brassica juncea* nonexpressor of pathogenesis related genes 1 (BjNPR1) exhibit resistance to downy mildew disease. PLoS One 9:e90839
39. Thakur R, Shetty H, Khairwal I (2006) Pearl millet downy mildew research in India: progress and perspectives. Int Sorghum Millets Newsl 47:125–130
40. Prabhu S, Kini R, Raj S et al (2012) Polygalacturonase-inhibitor proteins in pearl millet: possible involvement in resistance against downy mildew. Acta Biochim Biophys Sin 44:415–423
41. Prabhu S, Kini R, Shetty H (2012) Partial purification and characterization of polygalacturonase-inhibitor proteins from pearl millet. Afr J Biotechnol 11:7000–7008
42. Prabhu S, Singh R, Kolkenbrock S et al (2014) Experimental and bioinformatic characterisation of a recombinant polygalacturonase-inhibitor protein from pearl millet and its interaction with fungal polygalacturonases. J Exp Bot. doi:10.1093/jxb/eru266
43. Wagenknecht M, Meinhardt F (2011) Copy number determination, expression analysis of genes potentially involved in replication, and stability assays of pAL1—the linear megaplasmid of Arthrobacter nitroguajacolicus Ru61a. Microbiol Res 166:14–26
44. Favaron F, D'Ovidio R, Porceddu E, Alghisi P (1994) Purification and molecular characterization of a soybean polygalacturonase-inhibiting protein. Planta 195:80–87
45. Shevchenko A, Tomas H, Havlis J et al (2006) In-gel digestion for mass spectrometric characterization of proteins and proteomes. Nat Protoc 1:2856–2860
46. Edge A, Faltynek C, Hof L et al (1981) Deglycosylation of glycoproteins by trifluoromethanesulfonic acid. Anal Biochem 118:131–137
47. Anthon G, Barret D (2002) Determination of reducing sugars with 3-methyl-2-benzothiazolinonehydrazone. Anal Biochem 305:287–289
48. Deepak S, Shailasree S, Sujeeth N et al (2008) Serodiagnosis of pearl millet resistance to downy mildew by quantitating cell wall P/HRGP using polyclonal antiserum Pab-P/HRGP. Eur J Plant Pathol 121:77–85
49. Livak J, Schmittgen T (2001) Analysis of relative gene expression data using real-time quantitative PCR and the 2-ΔΔCt method. Methods 25:402–408
50. Préstamo G, Testillano P, Vicente O et al (1999) Ultrastructural distribution of a MAP kinase and transcripts in quiescent and cycling plant cells and pollen grains. J Cell Sci 112:1065–1076
51. Ceriotti A, Duranti M, Bollini R (1998) Effects of N-glycosylation on the folding and structure of plant proteins. J Exp Bot 49:1091–1103
52. Rozen-Gagnon K, Moreland N, Ruedl C, Vasudevan S (2012) Expression and immunoaffinity purification of recombinant dengue virus 2 NS1 protein as a cleavable SUMOstar fusion. Protein Expr Purif 82:20–25
53. Yao X, Li J, Deng N et al (2011) Immunoaffinity purification of α-momorcharin from bitter melon seeds (*Momordica charantia*). J Sep Sci 34:3092–3098
54. Albersheim P, Anderson-Prouty A (1975) Carbohydrates, proteins, cell surfaces, and the biochemistry of pathogenesis. Annu Rev Plant Physiol 26:31–52
55. Stotz H, Powell A, Damon S et al (1993) Molecular characterization of a polygalacturonase inhibitor from *Pyrus communis* L. cv. "Bartlett". Plant Physiol 102:133–138
56. Costa M, Costa J, Ricardo C (1997) A *Lupinus albus* root glycoprotein homologous to the polygalacturonase-inhibitor proteins. Physiol Plant 99:263–270
57. Faize M, Sugiyama T, Faize L, Ishii H (2003) Polygalacturonase-inhibiting protein (PGIP) from Japanese pear: possible involvement in resistance against scab. Physiol Mol Plant Pathol 63:319–327
58. Bergmann C, Cook B, Darvill A et al (1996) The effect of glycosylation of endopolygalacturonase and polygalacturonase-inhibitor protein on the production of oligo-galacturonides. Prog Biotechnol 14:275–282
59. Lim J-M, Aoki K, Angel P et al (2009) Mapping glycans onto specific N-Linked glycosylation sites of *Pyrus communis* PGIP redefines the interface for EPG-PGIP interactions. J Proteome Res 8:673–680
60. Solá R, Griebenow K (2009) Effects of glycosylation on the stability of protein pharmaceuticals. J Pharm Sci 98:1223–1245
61. Kemp G, Stanton L, Bergmann C et al (2004) Polygalacturonase-inhibiting proteins can function as activators of polygalacturonase. Mol Plant Microbe Interact 17:888–894
62. Machinandiarena M, Olivieri F, Daleo G, Oliva C (2001) Isolation and characterization of a polygalacturonase-inhibiting protein from potato leaves: accumulation in response to salicylic acid, wounding and infection. Plant Physiol Biochem 39:129–136
63. Nasmith C, Jeng R, Hubbes M (2008) Targeted gene analysis in *Ulmus americana* and *Ulmus pumila* tissues. For Pathol 38:90–103
64. Veronico P, Melillo M, Saponaro C et al (2011) A polygalacturonase-inhibiting protein with a role in pea defense against the cyst nematode *Heterodera goettingiana*. Mol Plant Pathol 12:275–287
65. Kalunke RM, Janni M, Sella L et al (2011) Transcript analysis of the bean polygalacturonase inhibiting protein gene family reveals that *Pvpgip2* is expressed in the whole plant and is strongly induced by pathogen infection. J Plant Pathol 93:141–148
66. Bezier A, Lambert B, Baillieul F (2002) Study of defense-related gene expression in grapevine leaves and berries infected with *Botrytis cinerea*. Eur J Plant Pathol 108:111–120

67. Lejeune A, Constant S, Delavault P et al (2006) Involvement of a putative *Lycopersicon esculentum* wall-associated kinase in the early steps of tomato-*Orobanche ramosa* interaction. Physiol Mol Plant Pathol 69:3–12
68. D'Ovidio R, Roberti S, Di Giovanni M et al (2006) The characterization of the soybean polygalacturonase-inhibiting proteins (PGIP) gene family reveals that a single member is responsible for the activity detected in soybean tissues. Planta 224:633–645
69. Tomassini A, Sella L, Raiola A, Favaron F (2009) Characterization and expression of *Fusarium graminearum* endo-polygalacturonases in vitro and during wheat infection. Plant Pathol 58:556–564. doi:10.1111/j.1365-3059.2008.02019.x
70. Oliver R, Ipcho S (2004) Arabidopsis pathology breathes new life into the necrotrophs-vs.-biotrophs classification of fungal pathogens. Mol Plant Pathol 5:347–352
71. Simon U, Bauer R, Rioux D et al (2005) The intercellular biotrophic leaf pathogen *Cymadothea trifolii* locally degrades pectins, but not cellulose or xyloglucan in cell walls of *Trifolium repens*. New Phytol 165:243–260
72. Sharada M, Shetty S, Shetty H (1995) Infection process of *Sclerospora graminicola* on *Pennisetum glaucum* lines resistant and susceptible to downy mildew. Mycol Res 99:317–322
73. Bergmann C, Ito Y, Singer D et al (1994) Polygalacturonase-inhibiting protein accumulates in *Phaseolus vulgaris* L. in response to wounding, elicitors and fungal infection. Plant J 5:625–634
74. Devoto A, Clark A, Nuss L et al (1997) Developmental and pathogen-induced accumulation of transcripts of polygalacturonase-inhibiting protein in *Phaseolus vulgaris* L. Planta 202:284–292
75. Di C-X, Li M, Long F et al (2009) Molecular cloning, functional analysis and localization of a novel gene encoding polygalacturonase-inhibiting protein in *Chorispora bungeana*. Planta 231:169–178
76. De Caroli M, Lenucci M, Di Sansebastiano G-P et al (2011) Protein trafficking to the cell wall occurs through mechanisms distinguishable from default sorting in tobacco. Plant J 65:295–308
77. Shi H, Zhu L, Zhou Y et al (2009) A cotton gene encoding a polygalacturonase-inhibitor-like protein is specifically expressed in petals. Acta Biochim Biophys Sin 41:316–324
78. Huang L, Liu Y, Yu X et al (2011) A polygalacturonase inhibitory protein gene (BcMF19) expressed during pollen development in Chinese cabbage-pak-choi. Mol Biol Rep 38:545–552
79. Kanai M, Nishimura M, Hayashi M (2010) A peroxisomal ABC transporter promotes seed germination by inducing pectin degradation under the control of ABI5. Plant J 62:936–947